Determination of velocity smoothing operator for prestack Kirchhoff depth migration using Common Scatter Point gathers

Hassan Khaniani and John C. Bancroft

ABSTRACT

Optimum smoothing is required in ray based prestack Kirchhoff depth migration to handle complex velocity models. It ensures numerical consistency and validity of modeling of finite difference data using ray tracing methods. Conventional approaches to find an optimum smoothing operator for the velocity field are based on visual inspection of final migrated image which is a time consuming and an expensive operation. In this work, to find an optimum smoothing operator, we propose to compare the modeled Common Scatter Point (CSP) data computed from ray tracing method with corresponding CSP gathers from real data.

For numerical analysis, we applied this approach for a scatterpoint within a highly complex structure of Marmousi 2-D synthetic dataset that were considered as the real data. For CSP modeling, the velocity of the Marmousi model was smoothed with four different smoothing operators (i.e., smoothing length of 50m, 150m, 250m and 500m). Then for each smoothed velocity, scatterpoint response from the coordination of (5500, 2450) m of the model were simulated by ray tracing. Comparing the ray tracing CSP gather with the real data showed that the smoothing length of 250 m had the most optimum fit among other smoothing lengths. Our modeling results are consistent with the optimum smoothing operator length published by Gray (2000) (i.e., 100 m-200 m) that were obtained based on visual inspection of the final depth migrated section.

INTRODUCTION

Figure 1 shows the relationship between reflection and diffraction traveltime surfaces in a common shot configuration. It shows that two scatterpoints R_1 and R_2on the reflector surface create two diffraction curves which are tangent to the reflection traveltime surface. The tangency between diffraction and reflection traveltime surface are a constructive interface. This is the basis for Kirchhoff migration algorithms (Claerbout, 1985, Yilmaz, 1987). Hence, in prestack Kirchhoff migration approach, it assumes the location of a scatter points within the geological model, and then gathers all appropriate energies from all available input traces and relocate it to the position of the scatter points (Bancroft, et al., 1996). Prediction of the diffractions traveltime response depends on waves propagating from sources location S to the scatterpoints R, and from scatterpoint R to the receivers. The CSP gather is an intermediate image gather in Equivalent Offset Migration (EOM). It is designed to collect all the possible diffraction energies based on a formulation that maps and sum the data with no time shifting (Bancroft et al, 1994, Margrave et al., 2001).

In the complex structures, prediction of diffraction traveltime curves is a challenging problem that can be approximated by ray tracing methods. One of the concerns in ray based methods is that the foundation of ray tracing techniques is based on the high frequency assumption of wave equation. Therefore, to be able to model seismic signals

by ray tracing, the spatial variations of velocity and its derivatives should be small with respect to the wavelength of the signal under consideration (Gray, 2000, Gajewski, et. al., 2002). This usually requires smoothing of the model. Smoothing is a process which also occurs in the propagation of real seismic waves since the earth serves as a low pass filter during propagation. (Gajewski, et. al., 2002) Thus an optimum smoothing of the velocity model is required to maintain consistency between the rays based data and the real seismic data.

In a study by Gray (Gray, 2000), he pointed out that appropriate smoothing is determined by optimizing between scattering of the rays, distorting the structure of the earth model, losing of the accuracy in the velocities, creating a poorer image and causing a depth shift in the resulting image. As an empirical criteria, Kramps (Kramps , 2003) suggested a maximum vertical velocity derivative of less than 50, and a horizontal one of less than 20 for depth migrations.

In both of the above approaches, optimum amount of velocity smoothing are found by the visual inspection of the final image after full prestack depth migration that are expensive and time consuming. We propose that optimum smoothing can be obtained by comparing the modeled CSP gathers with the real CSP gathers. One advantage of using the CSP gathers is that the data does not experience any time shifting in forming process, hence, it reduces some artifacts that are related to the time shifting. We implemented this approach on Marmousi 2-D synthetic dataset (Versteeg, 1994) and the results show that it is efficient and practical.

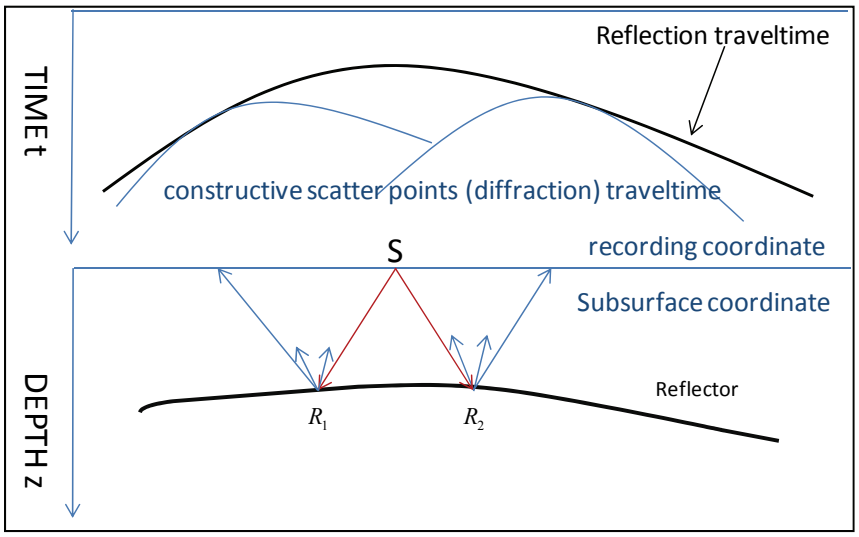

FIG. 1. Relationship between the reflection and the diffraction traveltime surfaces in a common shot configuration. Two scatterpoints on subsurface coordinate have constructive surface in the tangency point with reflection surfaces.

RAY TRACING ALGORITHM FOR THE CSP MODELING

Ray tracing methods are based on optical ray theory that is developed for seismic wave modeling (Cerveny, 1972, Cerveny, 2001). For an inhomogeneous general anisotropic medium, Cerveny (Cerveny , 1972) has derived the traveltime and amplitude

computation using asymptotic seismic ray tracing. His formulas are simplified for a seismic P-wave in an isotropic medium and elastic wave equation as (Chapman, 2004)

$$\nabla^2\Phi - \frac{1}{v^2}\frac{\partial^2\Phi}{\partial t^2} = 0, \tag{1}$$

where Φ represents the scalar potential of a P-wave. Assuming the high frequency approximation (i.e., $\omega \to \infty$) to the wave equation solution yields the Eikonal equation that describes the wavefront propagation at time $T(x,z)$ (see e.g. Popov 2002):

$$|\nabla \tau| = p, \tag{2}$$

where p is slowness. In Figure 2, if $\vec{x}$ represents the position vector of a point on a wavefront, and s is the path length of the curve traced out by this point as the wavefront evolves, then since both $d\vec{x}/ds$ and $\nabla\vec{T}/p$ are unit vectors parallel to the path, we have

$$\frac{d\vec{x}}{ds} = \frac{\nabla T}{p}. \tag{3}$$

Therefore, from equation (3) for 2D we have

$$\frac{dx_i}{dt} = v^2 p_i, \tag{4}$$

and

$$\frac{dp_i}{dt} = -\frac{1}{v}\frac{\partial v}{\partial x_i}, \quad i = 1,2. \tag{5}$$

To solve the ordinary differential equations (4) and (5) for ray tracing, we used 4th order Runge-Kutta method. Now, any scatterpoint response is modeled using the rays that depart from the scatterpoint into different directions (i.e., equally from -90 to +90 degrees with respect to the depth axis), then their traveltimes are recorded when the rays reach to the surface.

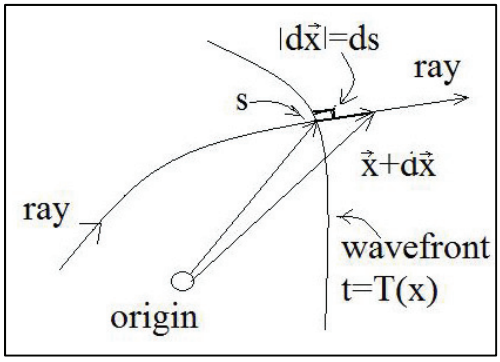

FIG. 2. Ray and wavefront (modified from Krebes, 2009)

Bancroft (Bancroft et al., 1994) introduced EOM as a prestack Kirchhoff time migration that maps the scatterpoint energies based on the Double Squares Root (DSR) equations into an equivalent offset (h_e) domain that is defined by

$$h_e = \sqrt{X^2 + h^2 - \left(\frac{2Xh}{tv_m}\right)^2}, \tag{6}$$

where, t is the two-way traveltime, X is the distance from input trace midpoint to the scatterpoint lateral coordination x, h is the half-offset between source and receiver and v_m is the migration velocity. In this process once the CSP gather is formed, to create final migrated image, it only requires a NMO stacking path. For a simple case where the lateral velocity variation is negligible, the NMO path is hyperbolic which is defined as (Bancroft et al., 1994, Margrave et al., 2001):

$$t(S,G) = \sqrt{t_0^2 + \left(\frac{2h_e}{v_m}\right)^2}, \tag{7}$$

where, t_0 is the zero offset two-way traveltime. Note that, if the geological model has strong lateral velocity change, the definition of formula (7) (collocation of the sources and the receivers) is not necessarily valid and the NMO stacking path can be found with ray tracing methods. In this situation, to simulate the CSP gathers, the traveltime response should be converted to a generalized equivalent domain by formula (7). In addition, as long as the equation(6) is valid, if any arbitrary source location be selected, the converted traveltime from offset domain to the equivalent offset domain will be arranged on a hyperbolic path. The reason for this fact is that the formation of any CSP gather is based on the distances from the source and receivers to the CSP location and not on the source/receiver offset. This is different in the complex structures, that equivalent offsets definition are approximate. As an example, Figure 3a shows the modeled scatterpoint response located at (5500 , 2450) m coordination of Marmousi velocity model in four different shot records. As expected in Figure 3b, the mapped shots record data to equivalent offset domain experience fluctuations. Therefore, the modeling process is more accurate when CSP data contains only information from adjacent shots and the average of modeled equivalent domain traveltimes are taken for analysis.

The CSP gathers of all Marmousi synthetic shot data at three different locations are shown in Figures 4-6. In all Figures, four scatterpoints are modeled and their traveltimes are plotted as blue dots. Here, we applied AGC on the gather for better illustration. Note that different amplitude scaling of two sides of the CSP gather happens for several reasons. The first reason is because of the acquisition parameters, that the survey was an "off end" survey with receivers to the left of the source being pulled towards the right. So, in the right side of sources, there is not any receiver to record the scattered energies that arrives to the surface. The second reason is the behaviour of wavefronts that has significant impacts on the amplitude. Because of complex model, the rays and wavefronts experience more caustics (i.e., the rays cross) and shadow zones (i.e., the area that the density of arriving rays to the surface are low) in right side of scatterpoints (see e.g., Figure 7).

Once the CSP modeling is performed, in a single image, we are able to compare it with the real CSP data and then obtain an optimum smoothing fit between them.

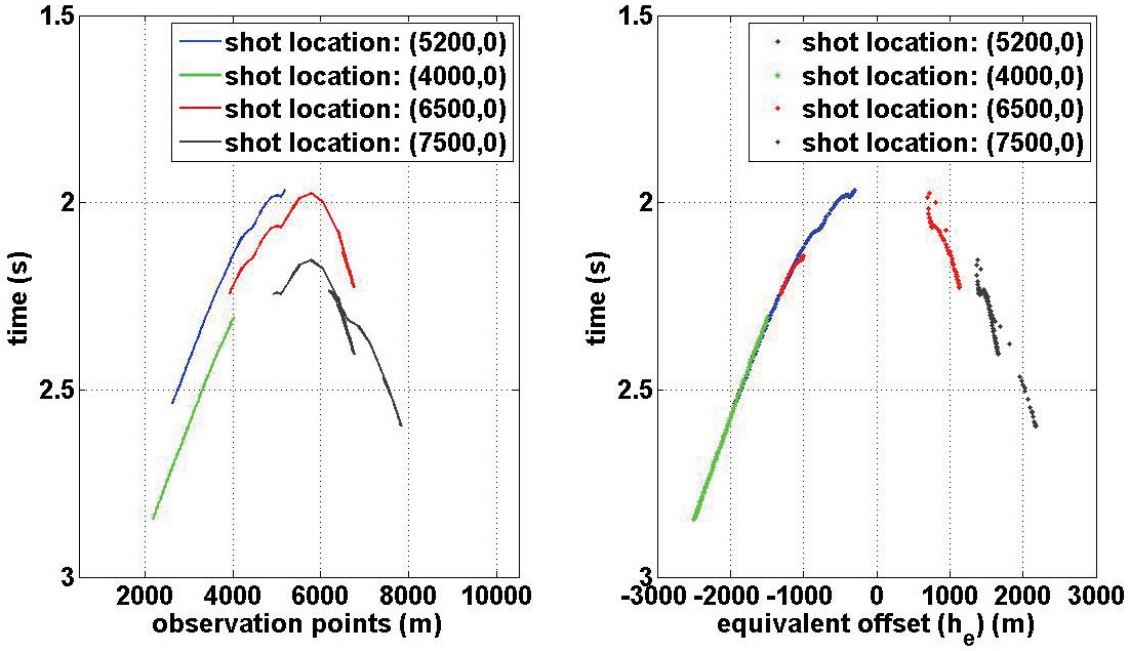

FIG. 3. Liability of CSP gathers modeling. One scatterpoint response at (5500, 2450) m of the model in four shot records by (a) location of involved receivers converted to (b) equivalent offset (h_e) domain.

NUMERICAL EXAMPLE IN OPTIMUM SMOOTHING

Ideally, optimum smoothing operator should be found for several coordination of the model. However, for our analysis, we selected a scatterpoint at coordination of (5500, 2450) m of the Marmousi velocity model. This scatterpoint is located within a highly complex structure zone of the model.

The modeling process was done by applying circular-shaped (Gaussian) smoothing operators with the lengths of 50 m, 150 m, 250 m and 500 m on Marmousi velocity model. The grid size of the velocity model was 12.5 m in both depth and lateral coordination. As described in (Appendix A), to preserve the traveltimes, in smoothing process for ray tracing, smoothing was done on the reciprocal of velocity (i.e., 1/v) instead of directly the velocity of the model. Then the traveltime response from the scatterpoint was simulated by tracing 300 rays that start from the scatterpoint and depart to the surface.

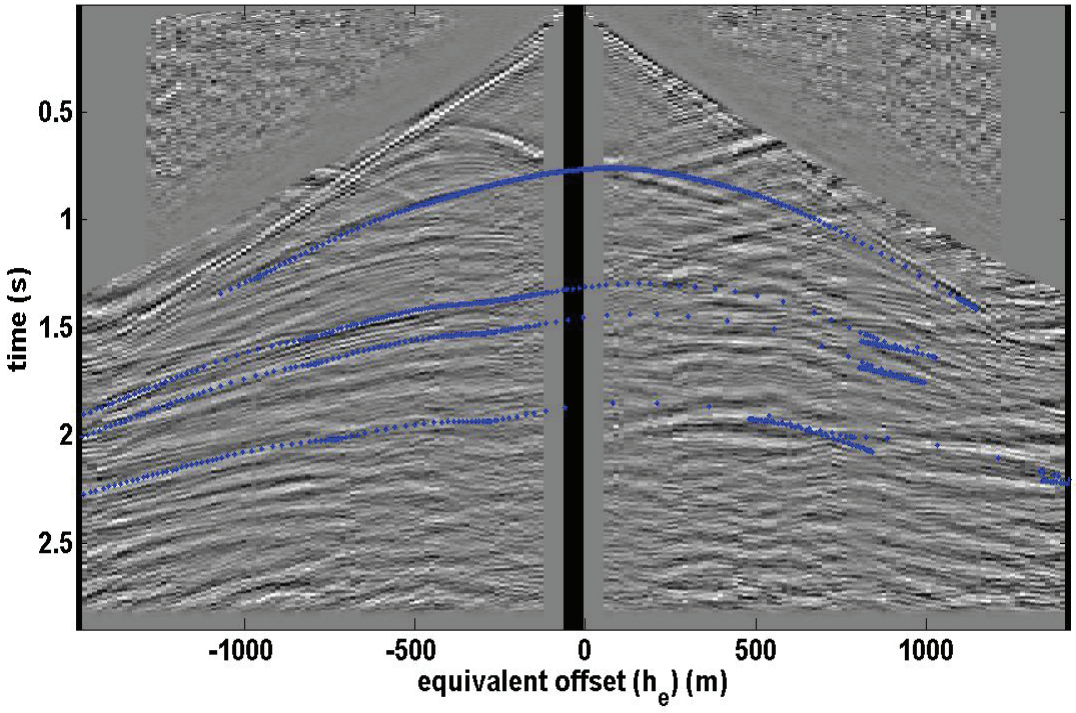

FIG. 4. Modeled traveltime and CSP gather formed at 5500 m from the left edge of the model. The blue traveltime curves are computed from scatter points located at depths of 790 m, 1550, 1755 and 2450m.

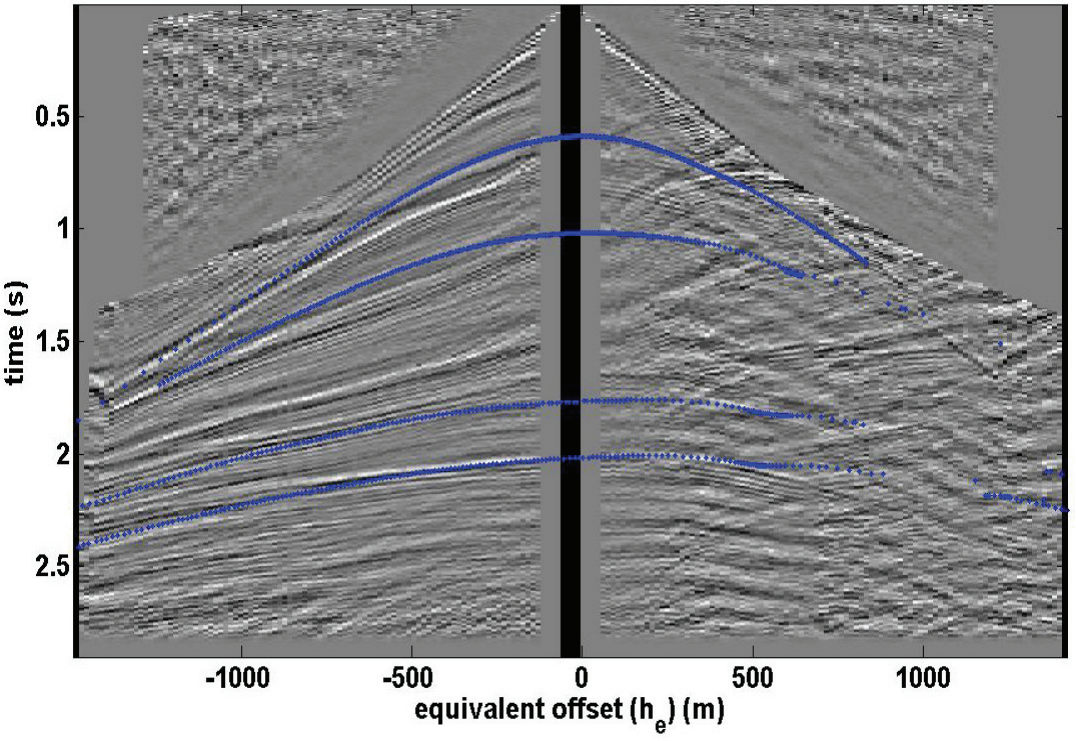

FIG. 5. Modeled traveltime and CSP gather formed at 4000 m from the left edge of the model. The blue traveltime curves are computed from Scatter points located at depths of 500 m, 950 m, 2000 m and 2335 m.

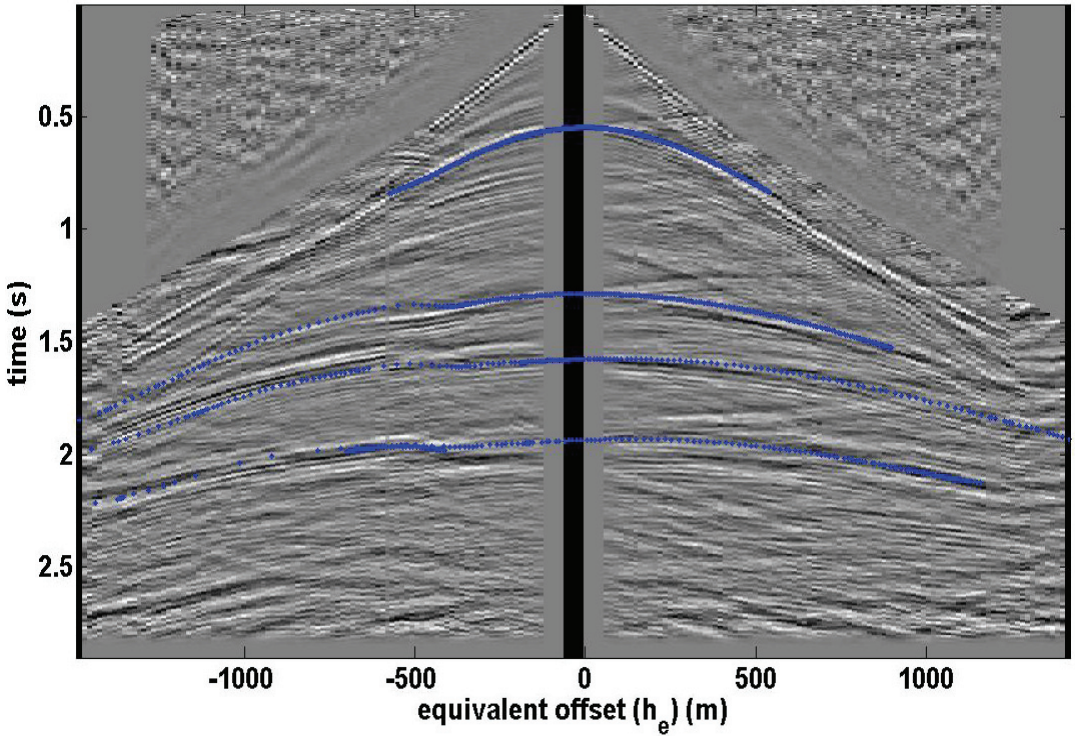

FIG. 6. Modeled traveltime and CSP gather formed at 7000 m from the left edge of the model. The blue traveltime curves are computed from scatter points located at depths of 470 m, 1335 m, 1800 m and 2320 m.

The wavefronts and their traveltime response are shown in Figures 7-8. They indicate that the different amounts of smoothing have different effects on the ray paths and wavefronts behaviours. To view the events on both sides of CSP gather accurately, the CSP gather formed with only 50 shots near the scatterpoint. The red arrows in Figure 9a show the expected scatterpoint response in the CSP gather from real data. Figure 9b shows that due to wild traveltime scattering and traveltime fluctuations the smoothing operator length from 50 m to 150 m are unstable and the modeled traveltimes are not consistent with the CSP data. As illustrated by the blue curve, by increasing the smoothing operator length to 250 m, optimum fit with CSP gather is obtained and fluctuations of modeled traveltime is less compared with 50m and 150 m. Modeling with the smoother length of 500 m is not desirable since large smoothing length caused a losing of accuracy in the velocities model and consequently the resolution of modeled traveltime.

This procedure should be repeated for several scatterpoints of the model. In Figures 4-6, for modeling of the traveltimes in the CSP gathers, different optimum smoothing operator lengths ranged from 150 to 250 were used. This shows that to obtain an optimum migrated image, optimum smoothing in several coordinations (i.e., lateral and vertical) are required.

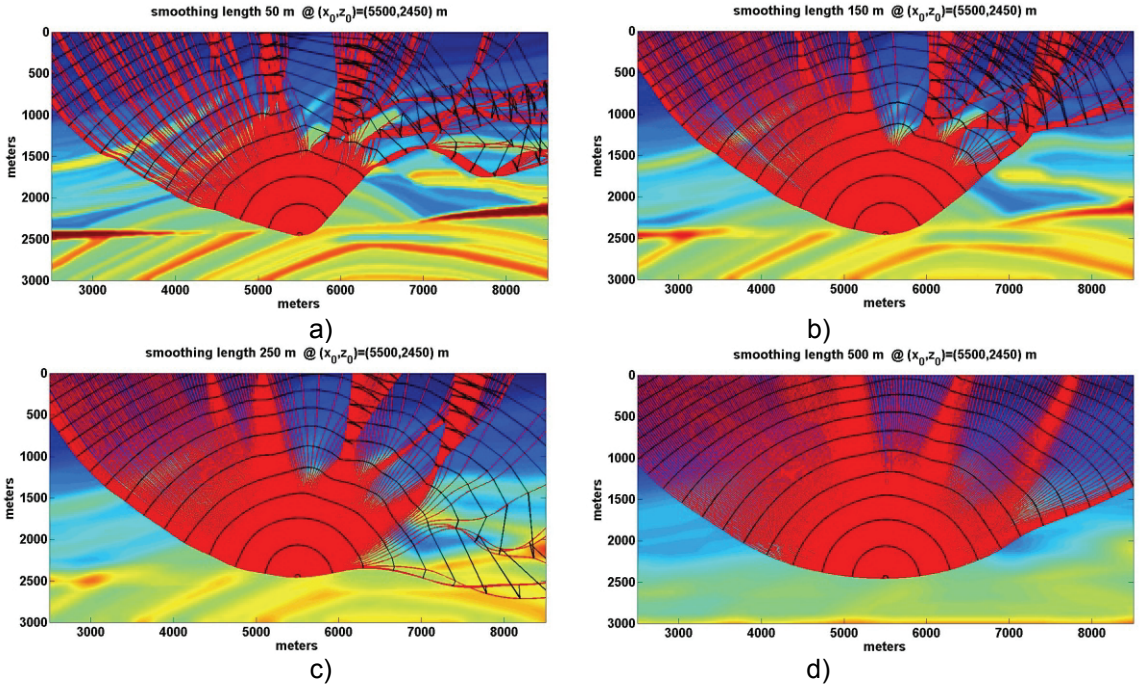

FIG. 7. Wavefront construction of a scatter point in Marmousi model at 5500 m lateral and 2450 m vertical coordination modeled by smoothing lengths of (a) 50 m (b) 150 m (c) 250 m (d) 500 m.

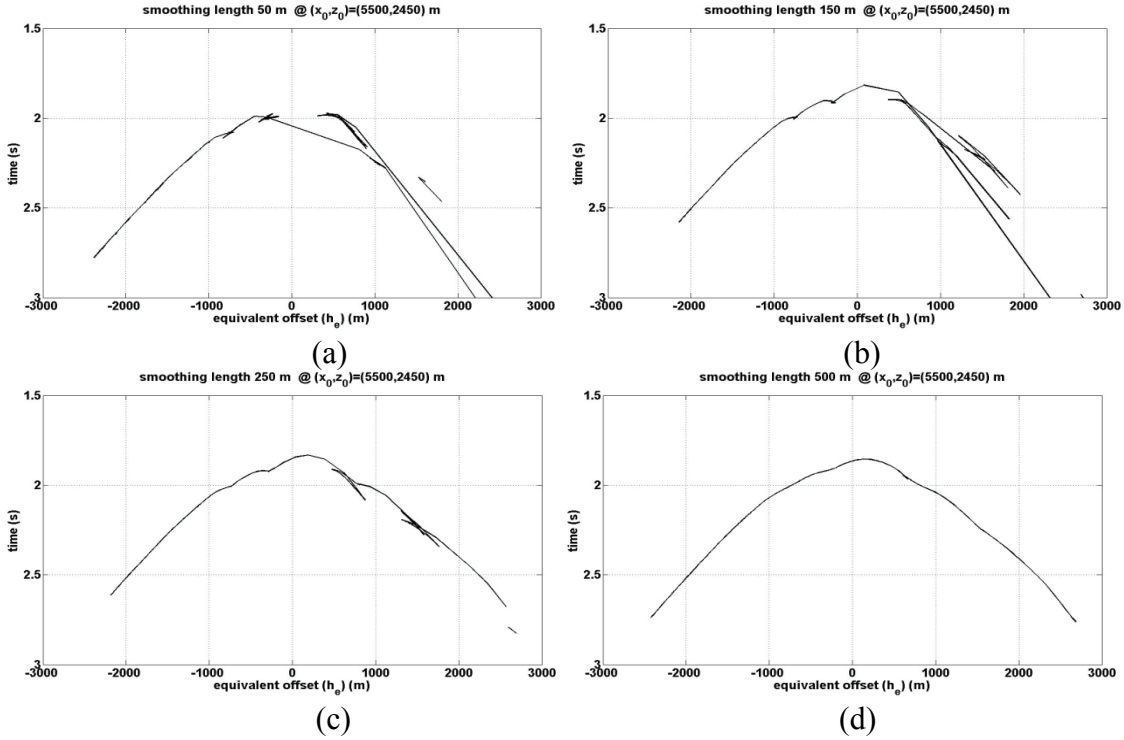

FIG. 8. Effects of smoothness on traveltime computation. Traveltime from a scatterpoint located at 5500 m lateral coordination and depth of 2450 is modeled by (a) smoothing length of 50 m (b) smoothing length of 150 m (c) smoothing length of 250 m and (d) smoothing length of 500 m.

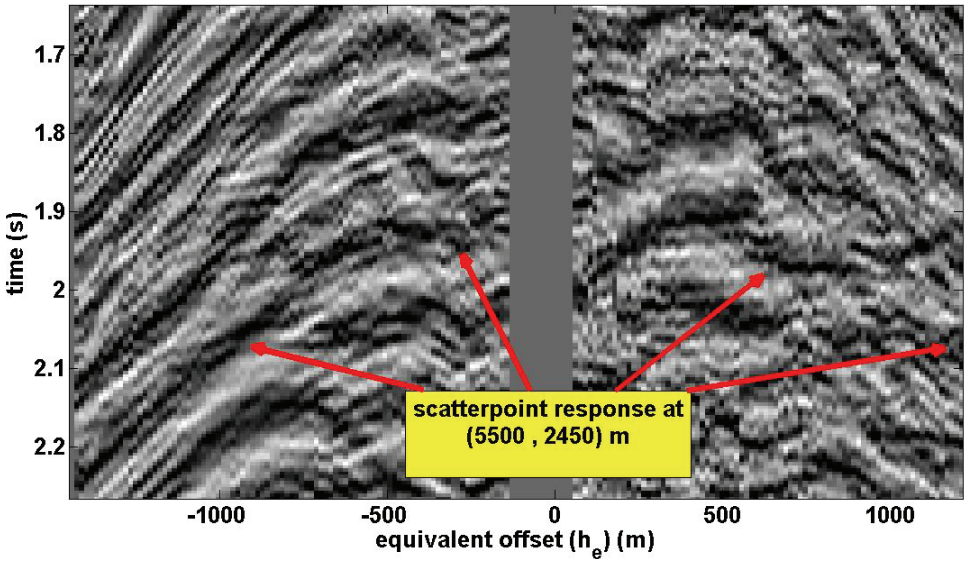

(a)

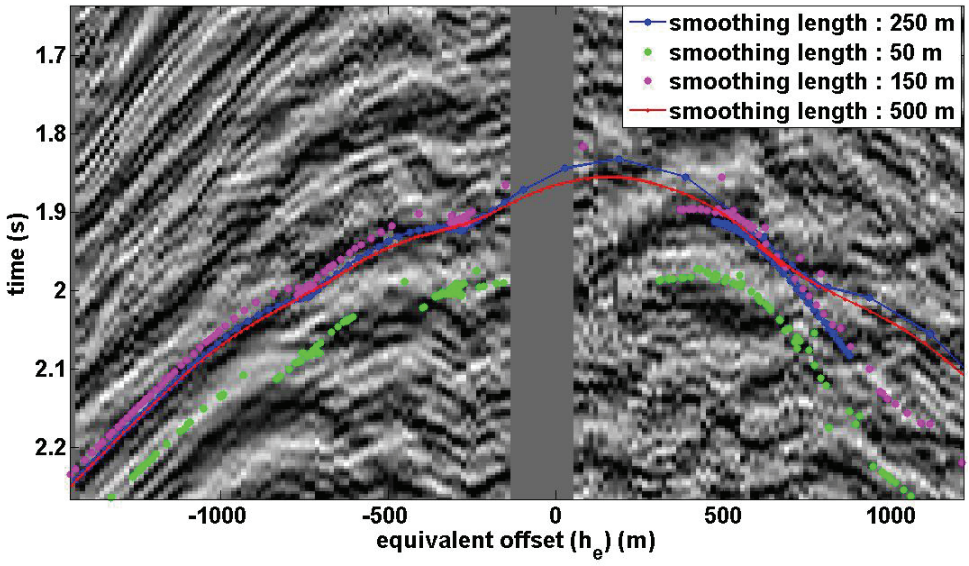

(b)

FIG. 9. Modeled traveltime and CSP gather formed at 5500 m from the left edge of the Marmousi model. As shown by red arrows in (a) an event caused by a scatterpoint response at depths of 2450 m is compared with (b) four modeled traveltime curves with different smoothing operators. The blue curve is an optimum fit.

CONCLUSIONS

We showed that the properties of CSP gather as a side product of equivalent offset migration (EOM) can serve as an efficient tool for determining the optimum smoothness of velocity model for prestack Kirchhoff depth migration. This is done by comparing the modeled scatterpoint traveltimes (which were achieved by ray tracing method) and corresponding CSP gathers from the Marmousi model (which the synthetic seismograms

were computed by the finite difference method). Hence, instead of visual inspection of full prestack migrated image, we are able to investigate required smoothing operator by CSP gathers image for every location within the model.

ACKNOWLEDGMENT

The authors would like to thank all CREWES sponsors, staff and students for their support. The comments of Dr. Mostafa Naghizadeh and Dr. Edward S. Krebes on ray theory and velocity smoothing methods are very much appreciated.

REFERENCES

Audebert, F., Biondi, B., Lumley, D., Nichols, D., Rekdal, T., and Urdaneta1, H., 2001, Marmousi traveltime computation and imaging comparisons, Stanford Exploration Project, Report 80.

Bancroft, J.C., 1996, Velocity sensitivity for equivalent offset prestack migration, Ann. Mtg: Can. Soc. Of Expl Geophys.

Bancroft, J. C., Geiger, H. D., and Margrave, G. F., 1998, The equivalent offset method of prestack time migration: Geophysics, **63**, 2042-2053.

Bancroft, J. C., Geiger, H. D., Foltinek, D. S., and Wang, S., 1994, Prestack migration by equivalent offsets and CSP gathers, CREWES 1994 Research Report.

Chapman, C. H. (2004), Fundamentals of seismic wave propagation (Cambridge University Press, Cambridge)

Cerveny, V., 2001, Seismic Ray Theory, Cambridge University Press.

Cerveny, V.,1972, Seismic rays and rays intensities in inhomogeneous and anisotropic media: Geophysics J. R. Astr. Soc. **29** 1-13.

Claerbout, J. F., 1985, Imaging the earth interior: Blackwell scientific publications.

Deregowski, S., and Rocca, F., 1981, Geometric optics and wave theory of constant offset sections in layered media: Geophys. Prosp., **29**, 374–406.

Gajewski, D., Coman R., and Vanelle C., 2002, Amplitude preserving Kirchhoff migration: a traveltime based strategy: Stud. geophys. geod., **46**, 193−211

Gray, S., 2000, Velocity smoothing for depth migration: How much is too much?, 70th Ann. Internat. Mtg: Soc. of Expl. Geophys., 1055-1058.

Kyoung J. L., 2005, Efficient Ray tracing algorithms based on wavefront construction and model based interpolation method, Phd. Thesis, Texas A&M University

Kamps, B., Smoothing velocities for depth migration, unpublished report, Tsunami Development. http://www.tsunamidevelopment.com

Krebes, E. S., 2009, Theoretical seismology, lecture notes: university of Calgary

Marchand, P., and Marmet, L., 1983, Binomial smoothing filter: A way to avoid some pitfalls of least square polynomial smoothing, Rev. Sci. Instrum., **54**, 1034-41, 1983.

Margrave, G. F., Bancroft, I. C. and Geiger, H. D, 1999. Fourier prestack migration by equivalent wavenumber: Geophysics, **64**, 197-207.

Pacheco, C., and Larner , K., Velocity smoothing before depth migration: Does it help or hurt? unpublished report, Center for Wave Phenomena, Department of Geophysics, Colorado School of Mines

Popov, M. M., 2002, Ray theory and Gaussian beam method for geophysicists: Salvador: EDUFBA.

Versteeg, R. J., 1993, Sensitivity of prestack depth migration to the velocity model: Geophysics, **58**, 873-882.

Versteeg, R. J., 1994, The Marmousi experience: Velocity model determination on a synthetic complex data set, Rice University

Yilmaz, Ö., 1989, Velocity-stack processing: Geophys. Prosp., **37**, 357-382.

APPENDIX A: SMOOTHING AND ITS CONSEQUENCE

The weighted moving average smoothing process works as a process that simply replaces each data value with the average of neighbouring values according to its weights

$\{w_1, w_2 \ldots, w_k\}$ such that $\sum_{n=1}^{k} w_n = 1$. These weights are used to calculate the smoothed data (S_t) (Marchand, et al., 1983),

$$S_t = \sum_{n=1}^{n} w_n x_{t+1-n} = w_1 x_t + w_2 x_{t-1} + \ldots + w_k x_{t-k+1}. \tag{A.1}$$

Mathematically, smoothing is a type of convolution; it is designed to reduce the data derivatives. Figure 10 shows a sample circular-shaped (Gaussian) operator for 200 m smoother that is obtained by spatial convolving a boxcar function with itself five times. Spatial convolution of this operator with the original model will smooth the model.

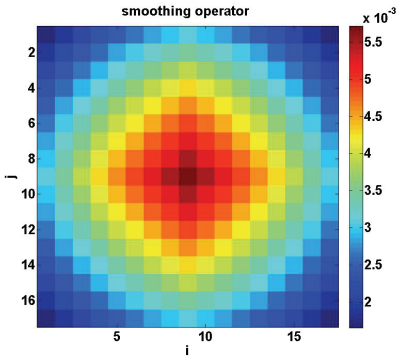

FIG. 10. A sample circular-shaped (Gaussian) smoothing operator

In smoothing the models for ray tracing, smoothness should be performed with the slowness models to maximally preserve the traveltimes. To illustrate this process, suppose that we have *n* horizontal velocity layers that are evenly spaced. Traveltime estimated by a smoothed slowness ($t_{slowness}$) is calculated by

$$t_{slowness} = \frac{\sum_{i=1}^{n} (\Delta z_i)}{n} \sum_{i=1}^{n} \frac{1}{v_i}, \tag{A.2}$$

where v_i is interval velocity of i^{th} layer, and Δz is depth interval. The traveltime estimated by a smoothed velocity ($t_{velocity}$) is

$$t_{velocity} = \sum_{i=1}^{n} (\Delta z_i) \times \frac{n}{\sum_{i=1}^{n} v_i}. \tag{A.3}$$

In Figure 11, equations (A.2) and (A.3) are numerically compared. It shows that $t_{velocity}$ is smaller than $t_{slowness}$. It also shows that $t_{slowness}$ is closer to true traveltime that for this model is

$$t_{true} = \sum_{i=1}^{n} \frac{\Delta z_i}{v_i} \tag{A.4}$$

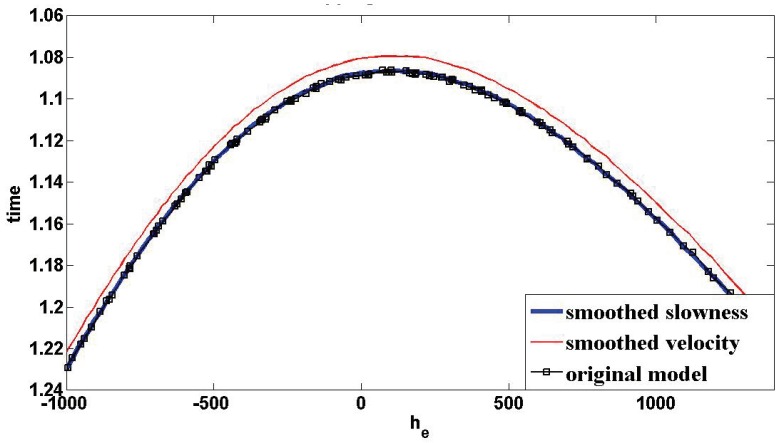

FIG. 11. Comparison of the modeled traveltime obtained from smoothed slowness and smoothed velocity The black traveltime curve is desired response, the blue curve is traveltime computed by smoothed slowness and the red curve is traveltime computed by smoothed velocity.